

Radio observations of massive stars

Ronny Blomme

Royal Observatory of Belgium, Ringlaan 3, B-1180 Brussel, Belgium

Abstract: Detectable radio emission occurs during almost all phases of massive star evolution. I will concentrate on the thermal and non-thermal continuum emission from early-type stars. The thermal radio emission is due to free-free interactions in the ionized stellar wind material. Early ideas that this would lead to an easy and straightforward way of measuring the mass-loss rates were thwarted by the presence of clumping in the stellar wind. Multi-wavelength observations provide important constraints on this clumping, but do not allow its full determination.

Non-thermal radio emission is associated with binarity. This conclusion was already known for some time for Wolf-Rayet stars and in recent years it has become clear that it is also true for O-type stars. In a massive-star binary, the two stellar winds collide and around the shocks a fraction of the electrons are accelerated to relativistic speeds. Spiralling in the magnetic field these electrons emit synchrotron radiation, which we detect as non-thermal radio emission. The many parameters that influence the resulting non-thermal radio fluxes make the modelling of these systems particularly challenging, but their study will provide interesting new insight into massive stars.

1 Introduction

Radio emission in massive stars occurs in almost all stages of stellar evolution. It starts with the molecular clouds in which the stars are formed: these can be detected in the radio through their maser emission (Elitzur 1992, Chapt. 8; Van der Walt, these proceedings). As the H II region forms, we can detect it in its atomic recombination lines, as well as in its thermal and non-thermal continuum emission (Rohlf & Wilson 2000, Chapt. 10 & 13). In the red supergiant phase, molecular maser emission again dominates (Elitzur 1992, Chapt. 8). During the Luminous Blue Variable (LBV) phase, the ionized material in the nebula emits at radio wavelengths (Umana et al. 2010; Umana, these proceedings). At the end-phase of evolution, compact objects are responsible for the radio emission in pulsars, massive X-ray binaries and micro-quasars (Paredes 2009). Various interactions with the interstellar medium, such as bowshocks, bubbles and supernova remnants are also detectable in radio emission (Rohlf & Wilson 2000, Chapt. 10; Cappa et al. 2002). The present review, however, will concentrate on the main-sequence evolutionary phase, as well as on the blue supergiant and Wolf-Rayet (WR) phases, where the radio emission is due to the thermal and non-thermal processes in stellar winds.

1.1 History

Historically, the first massive star detected at radio wavelengths was the LBV star P Cygni. Wendker et al. (1973) found fluxes of 9 ± 2 mJy¹ at 6 cm and 15 ± 3 mJy at 3 cm. Later, Wendker et al. (1975) were the first to detect a Wolf-Rayet star, WR 136, while studying its ejecta nebula NGC 6888. The first radio-detected O-type star was, not surprisingly, ζ Pup (Morton & Wright 1978).

In 1981, the 27-telescope Very Large Array (VLA²) became available, which presented a major step forward compared with the single-dish telescopes that had been used till that time. The 27 antennas not only provide a larger collecting surface area, but they are furthermore used as a radio interferometer. In such an interferometer, the spatial resolution is determined by the largest distance between two antennas. The positions of the VLA antennas are changed approximately every trimester, allowing astronomers to study the radio sky with different spatial resolutions. The high sensitivity of the VLA allowed Bieging et al. (1982) to make a survey of Wolf-Rayet stars (they detected 8 of the 13 stars studied). Later, Bieging et al. (1989) also surveyed OB stars, detecting 18 of the 88 stars studied.

1.2 Theory

In parallel, there were also theoretical developments in understanding and modelling the origin of the radio emission from these hot, massive stars. Within a very short time span various authors deduced that the emission is due to free-free processes in the ionized material of the stellar winds (Seaquist & Gregory 1973; Olon 1975; Panagia & Felli 1975; Wright & Barlow 1975). Working out the details, a simple equation is found that relates the radio flux (S_ν) to the mass-loss rate (\dot{M} , in $M_\odot \text{ yr}^{-1}$):

$$S_\nu = 2.24 \times 10^{11} \frac{1}{D^2} \left(\frac{\dot{M}}{\mu v_\infty} \right)^{4/3} \left(\frac{\gamma g Z^2}{\lambda} \right)^{2/3} [\text{mJy}], \quad (1)$$

where D is the distance to the star (in kpc), v_∞ is the terminal wind velocity (km s^{-1}), λ is the radio wavelength (cm) and g is the Gaunt factor. The chemical composition of the wind is encoded in the μ factor, and the ionization state in the γZ^2 factors. Eq. 1 suggests that radio observations are an easy way to determine mass-loss rates: we do not need to know the detailed ionization balance of some trace species (as we need for the analysis of ultraviolet P Cygni profiles), but only the gross ionization properties of the wind. We also do not need to know the shape of the velocity law (as we do need for H α , infrared and millimetre work), but only the terminal velocity.

The radio flux shows a near-power law dependence on the wavelength. Taking into account the weak wavelength dependence of the Gaunt factor, we have that $S_\nu \propto 1/\lambda^{+0.6}$, where the exponent $\alpha = +0.6$ is called the spectral index. It is also important to realize that the geometric region from which we receive the radio emission is quite extended. For an O-type star such as ζ Pup, the 6-cm formation region is beyond $\sim 100 R_*$. Furthermore, this region depends on the wavelength, because the optical depth for free-free absorption is proportional to λ^2 . At longer wavelengths, the formation region is formed further away from the star.

1.3 Non-thermal emission

Although the radio emission for most early-type stars is due to free-free emission, it became clear already early on that a number of anomalies exist. Abbott et al. (1980) found that the radio mass-loss

¹1 mJy = $10^{-29} \text{ W m}^{-2} \text{ Hz}^{-1} = 10^{-26} \text{ erg cm}^{-2} \text{ Hz}^{-1} \text{ s}^{-1}$.

²<http://www.vla.nrao.edu/>

rate for the O4 V star 9 Sgr was a factor 40 higher than that derived from the ultraviolet or $H\alpha$ line profiles. Such a difference is much higher than can be accounted for by the intrinsic errors. From spatially resolved observations, it is also possible to derive a brightness temperature (or a lower limit, if the source is unresolved). The brightness temperature of Cyg OB2 No. 9 was found by White & Becker (1983) to be higher than 300,000 K. It is very unlikely, however, that the electrons and ions responsible for the free-free emission would be at so high a temperature. Abbott et al. (1984) found flux variability in 9 Sgr and Cyg OB2 No. 9 which was too high to be attributed to changes in the stellar wind parameters. They also measured radio flux values that deviate significantly from the +0.6 spectral index, with values of $\alpha \approx 0.0$, or even negative in later observations (Bieging et al. 1989). All this indicates that, besides the free-free emission, a second mechanism is operating in these stars, which we call non-thermal emission.

2 Thermal radio emitters

Eq. 1 has been used to determine the mass-loss rates of hot, massive stars. One example is the large set of Wolf-Rayet mass-loss rate determinations by Cappa et al. (2004). The equation has also been used to study the mass-loss rate across the bi-stability jump (Benaglia et al. 2008). Theoretical modelling predicts a change in ionization around 21,000 K that substantially changes the mix of lines responsible for the radiative driving of the wind. The radio observations indeed indicate that around the bi-stability jump, stellar winds have a higher efficiency than expected from the general declining trend towards later spectral types.

2.1 Clumping

The major problem with Eq. 1, however, is that it does not include the effect of clumping or porosity. Many indicators show the presence of substantial clumping in stellar winds: the Phosphorus V discrepancy, X-ray spectroscopy, the electron scattering wings of WR emission lines, the presence of subpeaks on WR emission lines that are seen moving outward, ... (Crowther 2007; Puls et al. 2008). Also from a theoretical point of view, considerable clumping is expected due to the instability of the radiation driving mechanism of the stellar wind (Owocki & Rybicki 1984).

Because free-free emission is a process that depends on the density-squared, it is influenced by this clumping. Eq. 1 can be extended to include some simple model of clumping that assumes all the wind material is concentrated in clumps, with no interclump material. All clumps have the same clumping factor given by $f_{cl} = \langle \rho^2 \rangle / \langle \rho \rangle^2$, where the angle brackets indicate an average over the volume in which the radio continuum at that wavelength is formed. The resulting equation is (Abbott et al. 1981):

$$S_\nu = 2.24 \times 10^{11} \frac{1}{D^2} \left(\frac{\dot{M} \sqrt{f_{cl}}}{\mu v_\infty} \right)^{4/3} \left(\frac{\gamma g Z^2}{\lambda} \right)^{2/3}. \quad (2)$$

Sometimes, in the literature, a volume filling factor f is used. With our assumption of no interclump material, there is a direct relation between f and the clumping factor: $f = 1/f_{cl}$. In the above equation we have also assumed that the clumps are optically thin; optically thick clumps would result in porosity (Owocki et al. 2004).

Eq. 2 considerably changes the interpretation of an observed radio flux. All we can derive from the observations is the combined quantity $\dot{M} \sqrt{f_{cl}}$. A given flux can thus correspond to a certain mass-loss rate assuming a smooth wind ($f_{cl} = 1$), or to a lower mass-loss rate assuming a clumped wind ($f_{cl} > 1$). This uncertainty in the mass-loss rates has important consequences for stellar evolution: if the

rates during the main-sequence evolution are too low, mass-loss episodes during other evolutionary phases need to be invoked to explain the existence of Wolf-Rayet stars (Smith & Owocki 2006).

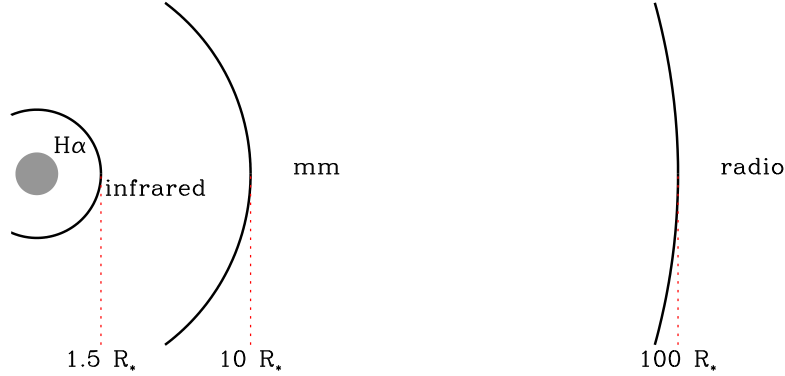


Figure 1: The formation regions of various density-squared observational indicators in the stellar wind of a typical O-type star.

2.2 Clumping gradients in OB stellar winds

From radio data alone, it is difficult to make a distinction between smooth and clumped winds. But a number of other observational indicators are also sensitive to clumping because they depend on density-squared processes (as does the radio emission). These indicators include the $H\alpha$ spectral line, the infrared and the millimetre continuum. Interestingly, these different indicators are formed in different regions of the wind (Fig. 1). Very approximate values for an O-type star with a strong stellar wind are: $H\alpha$ within $1.5 R_*$ of star, infrared up to a few R_* , millimetre from about $10 R_*$ and radio from $\sim 100 R_*$.

This opens up the possibility to compare the clumping in different regions of the wind, and to see if there is a gradient in the clumping. Lamers & Leitherer (1993) were the first to attempt this, by comparing the mass-loss rate derived from the $H\alpha$ line with that from the radio (assuming a smooth wind). They found no significant differences and therefore concluded that significant clumping in stellar winds was unlikely.

Runacres & Blomme (1996) compared the infrared, millimetre and radio fluxes with smooth wind models for a sample of 18 OB stars. The models were fitted through the observed visual and near-infrared continuum fluxes, which fixes the distance and interstellar extinction. They determined the mass-loss rate so that a good fit to the observed radio fluxes was also obtained. They then checked how well this smooth wind model agreed with the observed far-infrared and millimetre fluxes (which were not used in the fitting procedure). Four stars (α Cam, δ Ori A, κ Ori and ζ Pup) show fluxes that are significantly higher than the smooth wind model.

Later, an even better example was found: for the bright B0 Ia star ϵ Ori, Blomme et al. (2002) combined new data with archival observations and applied the same technique. Fig. 2 shows the observed fluxes as a function of wavelength, covering the range from visual to radio wavelengths. The y-axis shows the observed flux divided by the smooth wind flux. Any significant excess above the $y=1$ line is interpreted as being due to clumping in the wind. A clear excess is seen at millimetre wavelengths, with a possible onset already in the far-infrared and a continuation in the radio region. This indicates the presence of more clumping in the geometric region where the millimetre flux is formed.

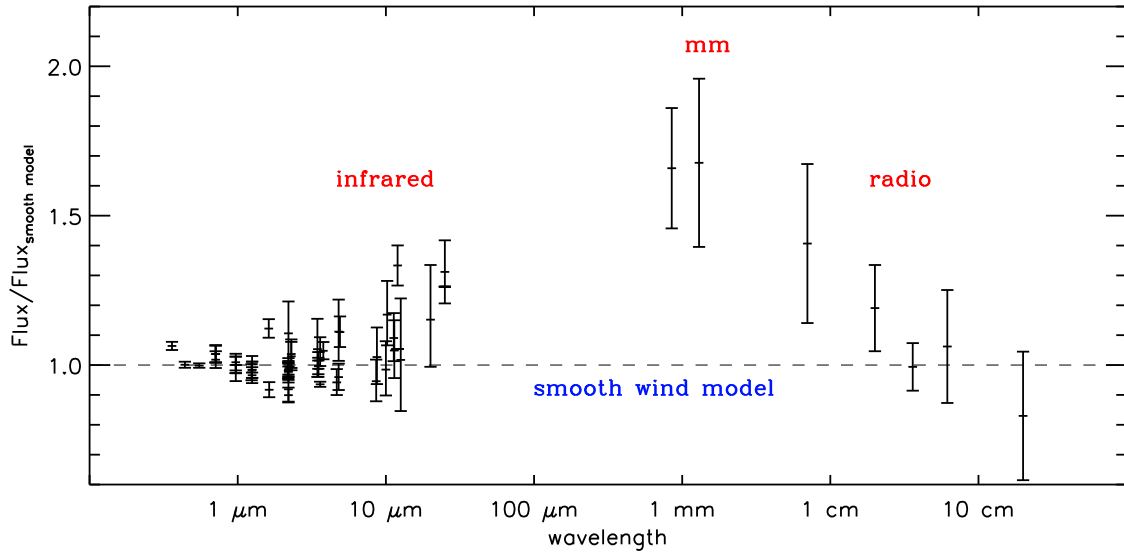


Figure 2: The ϵ Ori fluxes from visual to radio wavelengths, compared with a smooth wind model. The flux excess in the millimetre region is interpreted as indicating a higher clumping factor in the millimetre formation region. Based on Blomme et al. (2002), with some new radio data added.

It is important to realize that in this type of work we need to assume that the wind region where the radio emission is produced, is not clumped, otherwise we would just introduce another parameter on which we have no observational constraints. But it is of course quite likely that the radio formation region is also clumped. The downward gradient seen in the 7 mm to 20 cm radio fluxes (Fig. 2) is suggestive of some decrease of clumping in the radio formation region, as we go further out in the wind.

Puls et al. (2006) not only studied the continuum fluxes, but also included the $H\alpha$ line, for a sample of 19 O-type supergiants and giants. The first thing they noticed is that the radio mass-loss rates (assuming a smooth wind) are in better agreement with the predicted wind-momentum luminosity relation (Vink et al. 2000) than the $H\alpha$ mass-loss rates (again, assuming a smooth wind). A closer inspection reveals that it is mainly the stars with $H\alpha$ in emission (i.e. those with a stronger stellar wind) that are most discrepant.

Puls et al. (2006) then introduced a clumped wind model. The wind was divided into 5 regions, and in each region a constant clumping factor was taken. These clumping factors were then adjusted to obtain a good fit to the observed $H\alpha$, infrared, millimetre and radio data. Because of the reason explained above, the radio region was assumed not to be clumped. A major result from their work is the behaviour of the clumping factor in the $H\alpha$ formation region (their Fig. 10). For stars with low mass-loss rates, the clumping factors are not significantly different from 1. But for stars with higher mass-loss rates, the $H\alpha$ clumping factors average around 4. This means that the geometric region where $H\alpha$ is formed (i.e. close to the stellar surface) is more clumped than the radio formation region, at least for OB stars with strong winds.

2.3 Clumping gradients in Wolf-Rayet stellar winds

Such a gradient in the clumping factor might also exist in Wolf-Rayet stars. Nugis et al. (1998) studied the spectral index between the infrared and radio wavelengths for 37 WR stars. According to Eq. 1, this spectral index should be $\alpha = +0.6$ for a wind that has the same clumping everywhere.

However, Nugis et al. measured α values from $+0.66 \pm 0.01$ up to $+0.88 \pm 0.04$, with most spectral indices being larger than $+0.7$ (their Fig. 1). This again indicates more clumping in the inner part of the wind compared with the outer part. Nevertheless, the interpretation of these results is more complicated than for OB stars, because the ionization in a Wolf-Rayet wind can change sufficiently to influence the spectral index. Furthermore, for at least one WR star, Montes et al. (these proceedings) ascribe the higher than $+0.6$ spectral index to thermal emission in the increased density region of a colliding-wind binary.

In summary, it is clear that OB stars with strong winds show a gradient in their stellar wind clumping, with stronger clumping in the inner part of the wind. Puls et al. (2006) also point out that these results are not in agreement with the hydrodynamical models of Runacres & Owocki (2005), which predict more clumping in the radio than in $H\alpha$. It is possible however that even minor changes in the input physics of these hydrodynamical models might change this conclusion. A similar clumping gradient probably also exists in the winds of Wolf-Rayet stars, with the important caveat that ionization changes also play a role which are not easy to distinguish from clumping.

3 Non-thermal radio emitters

In Sect. 1.3, we saw that some hot, massive stars also show non-thermal radio emission. This emission is characterized by a spectral index significantly smaller than the $+0.6$ value for thermal emission and by a high brightness temperature. It is also frequently associated with variability in the radio fluxes, though this characteristic in itself is not sufficient to identify non-thermal emission: e.g., the LBV P Cygni shows radio variability, but this is due to ionization changes in the wind, not to non-thermal emission (Exter et al. 2002).

In the literature, various values for the incidence of non-thermal emission are cited. Abbott et al. (1986) claim that 12 % of the Wolf-Rayet stars are non-thermal and Bieging et al. (1989) give at least 24 % of the OB stars. Later, much higher numbers were claimed: 20 – 30 % of the detected WR stars (Cappa et al. 2004); more than 40 % of the Wolf-Rayet stars (Leitherer et al. 1997; Chapman et al. 1999); up to 50 % of detected O-type stars (Benaglia et al. 2001). The reason for these differences is an observational bias: non-thermal emitters are intrinsically radio-brighter than thermal ones and therefore easier to detect. The higher percentages indicate the probability of finding a non-thermal emitter in a random sample of massive stars. The lower percentages by Abbott et al. (1986) and Bieging et al. (1989) refer to volume-limited samples, and therefore give a better indication of the incidence of non-thermal emission in massive stars.

3.1 Binary connection

Quite early on, it was clear that there was some connection between non-thermal emission and binarity. Moran et al. (1989) used the MERLIN radio telescopes to spatially resolve the emission from WR 147. They found a thermal radio emitting source at the position of the Wolf-Rayet star itself and also a well separated non-thermal source between the WR star and a close-by B-type star (this companion was discovered later in the infrared by Williams et al. 1997). The geometry of the situation suggests that the non-thermal region is positioned at the collision region between the wind of the Wolf-Rayet star and that of the B-type star.

A detailed theoretical explanation was provided by Eichler & Usov (1993). In a massive binary system, the stellar winds of both components collide (Fig. 3). This creates a contact discontinuity with a shock on either side. The position and shape of the contact discontinuity is determined by the relative strengths (ram pressure) of the two winds: the discontinuity is closer to the star with the weakest wind, and wraps around that star.

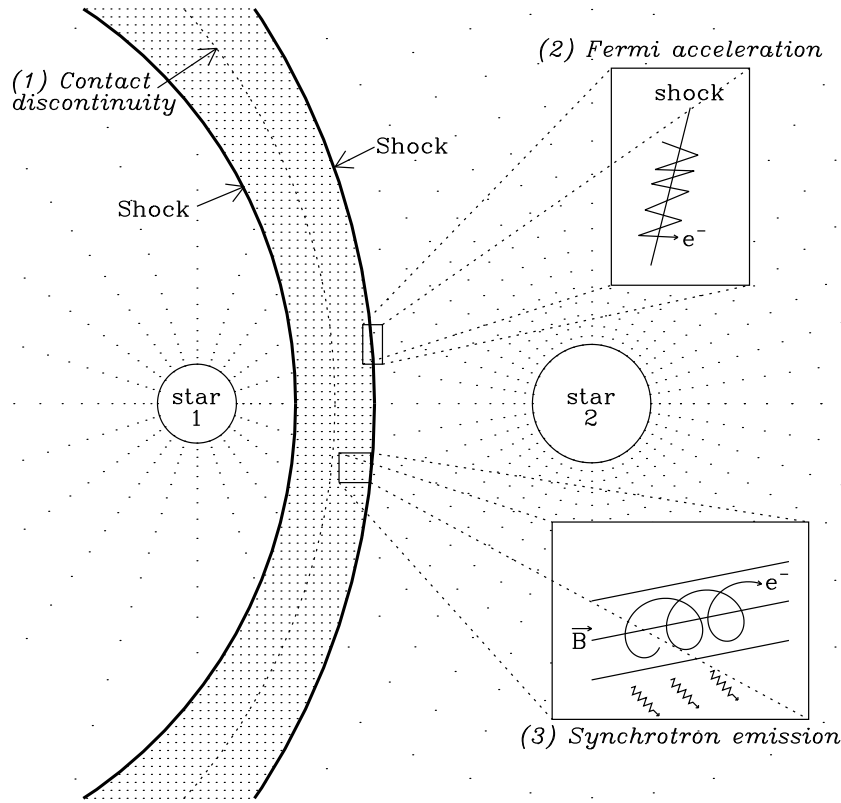


Figure 3: Synchrotron emission from colliding winds. (1) The winds of both components collide, creating a shock on either side of the contact discontinuity. (2) At each shock, the Fermi mechanism accelerates a fraction of the electrons to relativistic speeds. (3) These relativistic electrons spiral in the magnetic field and emit synchrotron radiation.

At each shock, a fraction of the electrons is accelerated up to relativistic speeds, through the first-order Fermi mechanism (Bell 1978). In this mechanism, electrons bounce back and forth across the shock and at each bounce gain some energy from the shock (Fig. 3). A fraction of the electrons make enough bounces to attain relativistic speeds. These electrons then spiral around in the magnetic field, emitting synchrotron radiation at radio wavelengths. It is this synchrotron radiation that we see as the non-thermal emission.

The synchrotron emission has a spectral index of -0.5 to -1.0 (Bell 1978; Pittard et al. 2006), explaining the observed spectral index. The emission is due to high-energy particles, which explains the high brightness temperature. Not all of the synchrotron emission is detected, however, because part of it (or in some cases, all of it) is absorbed by the free-free absorption in the stellar winds of both stars. The effect of the absorption depends on the orbital phase, because the sightline from the synchrotron emission region to the observer passes through different parts of the wind(s) as the positions of the stars change in their orbit. Furthermore, in an eccentric binary, the changing separation also generates variability in the intrinsic synchrotron emission as the ram pressure of the collision changes. The combination of both effects explains the variability seen in non-thermal radio emitters.

Van der Hucht et al. (1992) studied a number of Wolf-Rayet stars and found a good correlation between binarity and non-thermal emission. They also showed that these binaries are frequently associated with dust emission (detectable in the infrared) and with X-ray emission. They made the bold extrapolation “... that all other non-thermal WR stars discussed in this paper, as well as all (variable) non-thermal radio OB stars (...), are actually long-period binaries...”.

3.2 Wolf-Rayet binaries

An outstanding example of a colliding-wind binary is WR 140. It consists of a WC7 + O4-5 star in a 7.9-yr orbit with a high eccentricity ($e \approx 0.88$). White & Becker (1995) followed this system during more than one orbital period and determined the 2, 6 and 20 cm fluxes approximately every month. The detailed radio light curves (their Fig. 3) show substantial variability that is well correlated with orbital phase and that repeats from one orbit to the next. The light curves at different wavelengths are reasonably similar to one another, except that the shorter-wavelength curves start rising earlier and decline more slowly after maximum. The variability is due to the combined effect of changing synchrotron emission and free-free absorption as a function of orbital phase. Obtaining a good model fit to these data is still a considerable challenge (Pittard, these proceedings).

More recently, Dougherty et al. (2005) have used the Very Long Baseline Array (VLBA) to spatially resolve the wind-collision region. They obtained data with a resolution of ~ 2 milli-arcsec at 23 epochs, covering orbital phases 0.74 to 0.97. These data reveal how the emission region changes orientation and size as a function of orbital phase. The continued popularity of WR 140 is shown by the many contributions about this system at this colloquium (Dougherty et al.; Fahed; Parkin; Russell et al.; Sugawara et al.; Williams, these proceedings).

Although WR 140 is an outstanding example of the link between binarity and non-thermal emission, the link cannot be proven with only one, or a few, examples. A more statistical approach was taken by Dougherty & Williams (2000). From the 23 WR stars they studied, they selected 9 that had a non-thermal spectral index, or composite index (between thermal and non-thermal). Seven of these stars are known binaries (later, Marchenko et al. (2002) found WR 112 to have dusty spiral, strongly suggesting it is also a binary). A plot of the spectral index vs. orbital period (Dougherty & Williams, their Fig. 1) shows an interesting correlation: short-period stars have a nearly-thermal index, while long-period stars have a non-thermal index. This effect is easily explained with the colliding-wind model: short-period binary components are so close to one another that all synchrotron emission is absorbed by the free-free absorption region in the stellar winds. Longer-period binaries have components that are further away from one another; the synchrotron emitting region is therefore largely outside the free-free absorption, and most of the synchrotron emission gets through to the observer.

3.3 Single O stars

While the link between binarity and non-thermal emission is quite strong for Wolf-Rayet stars, this was not the case for O-type stars. Some years ago, there were still a number of non-thermal O stars that were seemingly single. Before getting carried away by the binary explanation, it is therefore important to also investigate if single stars can produce non-thermal emission. After all, there are shocks in the winds of single stars, due to the instability of the radiative driving mechanism (Owocki & Rybicki 1984), and these shocks should be able to accelerate electrons and thus generate synchrotron emission.

Van Loo et al. (2006) investigated this possibility for a typical O-star non-thermal emitter, Cyg OB2 No. 9. They made a model containing a number of shocks in the stellar wind. The parameters of these shocks (mainly the shock jump velocity) were inspired by the Runacres & Owocki (2005) hydrodynamical model. They then calculated the number of relativistic electrons accelerated at each shock and followed them as they cooled down due to inverse Compton and adiabatic cooling. From this, the synchrotron emission was calculated, and – taking into account the free-free absorption – the emergent radio flux was determined. There is considerable synchrotron emission in the inner part of the wind, where the shocks are strong (high jump velocity). This emission, however, is completely absorbed by the free-free absorption. In the outer part of the wind, there is also synchrotron emission, but the shock jump velocity has reduced considerably there, so there is not enough emission to

explain the observations. The fact that the model cannot explain the Cyg OB2 No. 9 observations throws serious doubt on the single-star hypothesis.

3.4 O star binaries

More positive proof that Cyg OB2 No. 9 is a binary was provided by Van Loo et al. (2008). Using VLA archive data covering 20 years, they detected a 2.355-yr period in the radio data (see also Volpi, these proceedings). The radio fluxes vary with orbital phase and the variations repeat very well from one orbit to the next. All this indicates that Cyg OB2 No. 9 is a binary. At the same time Nazé et al. (2008) also detected binarity in the spectroscopic data. Newer spectroscopic observations are presented in Nazé et al. (2010, and these proceedings).

A similar technique was used on HD 168112 observations by Blomme et al. (2005). The amount of data is less than for Cyg OB2 No. 9, so the result is less certain. A period between 1 and 2 years is found, with $P = 1.4$ yr as the formally best value. There is as yet no spectroscopic confirmation of the binary status of this star.

As we did for the Wolf-Rayet stars, we need to proceed to a more statistical approach to show the link with binarity. Detailed statistics of non-thermal emission in O-type stars are provided by De Becker (2007) and by Benaglia (2010). De Becker (his Table 2) shows that many of the O-star non-thermal emitters are now confirmed, or at least suspected, binaries. Although a few stars have not yet been investigated for multiplicity, we can now confidently confirm the Van der Hucht et al. (1992) quote (Sect. 3.1) that all non-thermal O-star and Wolf-Rayet star radio emitters are indeed colliding-wind binaries.

3.5 Remaining problems

Although the link between non-thermal emission and binarity is now quite secure, that does not mean we understand everything about non-thermal radio emission. One interesting point is that quite a number of non-thermal emitters are actually multiple systems. A nice example is HD 167971, which consists of a 3.3-d eclipsing binary and a third light (Leitherer et al. 1987). It is not clear if this third component is gravitationally bound to the binary, or whether it is just a line-of-sight object. Blomme et al. (2007) studied the VLA archive data of this system. They did not find any radio variability on the 3.3-day time scale, as may be expected from such a short-period binary. But the data show a clear cycle of ~ 20 yrs, suggesting that the third component and the binary are gravitationally bound and orbit each other with a 20-yr period. Another example of a multiple system is Cyg OB2 No. 5 (Kennedy et al. 2010; Dougherty, these proceedings).

A further problem is posed by the short-period binary Cyg OB2 No. 8A ($P = 21.9$ d, De Becker et al. 2004). Although no synchrotron emission was expected from such a close binary, the VLA data do show orbit-locked variability (Blomme et al. 2010; see also Fig. 4, left panel). This radio variability is furthermore nearly anti-correlated to the X-ray variability. Blomme et al. develop a theoretical model for this system, starting from an analytical solution for the position of the contact discontinuity. At both shocks, relativistic electrons are injected and followed as they move away with the flow and as they cool down due to adiabatic and inverse Compton cooling. The resulting synchrotron emission is then included in a radiative transfer calculation, together with free-free absorption, giving the radio flux. By following the two components along their orbit, an artificial light curve is constructed. A first model that uses the wind parameters determined by De Becker et al. (2006) fails to explain the observations. By accepting stellar wind parameters that are different from those expected for single stars, however, we achieve a better agreement (Fig. 4, right panel). The model can qualitatively explain many of the observed features of the radio data, as well as the anti-correlation with the X-ray

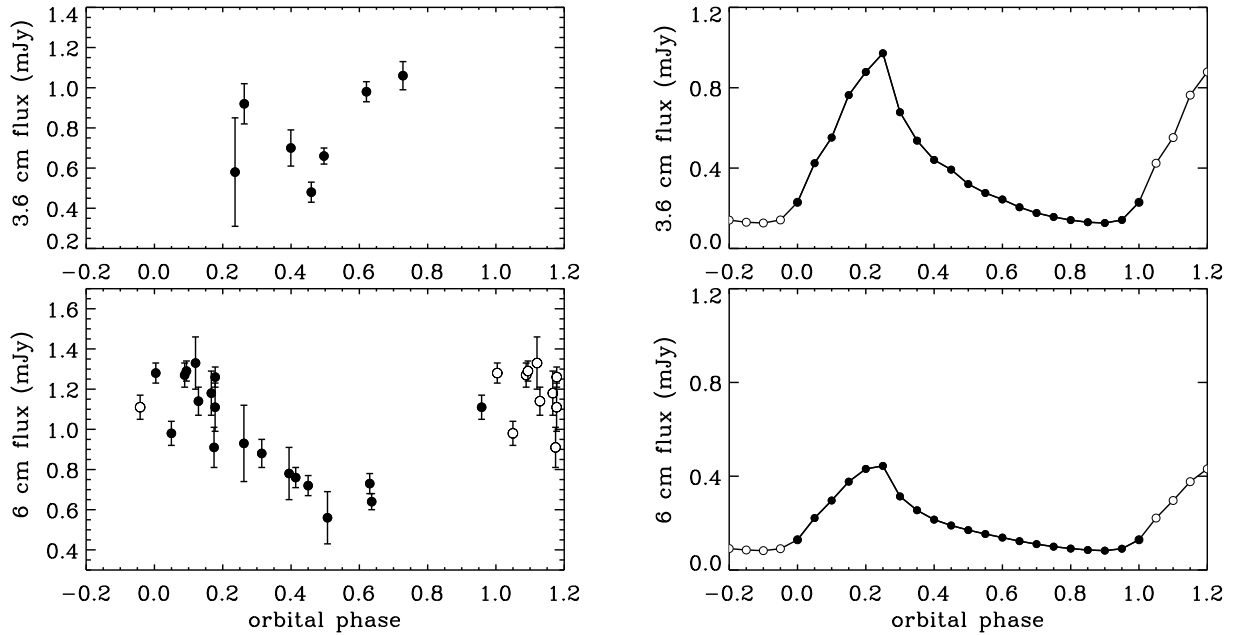


Figure 4: Observed (left panel) and calculated (right panel) radio fluxes for Cyg OB2 No. 8A. The phase range is extended by 0.2 on either side to provide a good overview of the variability. Open circles indicate duplication in this extended range. Phase 0.0 corresponds to periastron. From Blomme et al. (2010).

data. Problems remain with explaining the spectral index: the model values range between $+0.75$ and $+1.5$, while the observed value remains close to ~ 0.0 . Porosity is suggested as a possible solution for this problem.

Modelling these colliding-wind binaries can therefore tell us something about porosity in single-star winds. For this, we need detailed theoretical models, which is quite challenging work as the models need to explain not only the radio data, but also the X-ray and optical spectroscopy observations. A review of modelling colliding-wind binaries is given by Pittard (these proceedings).

4 Future radio astronomy

A number of existing radio facilities are currently being upgraded. The VLA is being converted into the EVLA³ (Dougherty & Perley, these proceedings), resulting in an order of magnitude improvement in sensitivity and a very large wavelength coverage. The MERLIN instrument is also being upgraded to e-MERLIN⁴. One of the legacy programmes planned for e-MERLIN is a deep radio survey of the Cyg OB2 association (PI: R. Prinja; see Willis et al., these proceedings). As Sect. 3 has made clear, Cyg OB2 has provided quite a number of colliding-wind binaries and these new data are expected to provide more examples, as well as many detections of thermal radio emission.

On the southern hemisphere, two interferometers are being constructed, one in South-Africa (MeerKAT⁵) and one in Australia (ASKAP⁶). Both will start with a modest number of telescopes, but MeerKAT will later be extended to 80 antennas (in 2013-2016), and ASKAP to 36 antennas

³<http://science.nrao.edu/evla/>

⁴<http://www.e-merlin.ac.uk/>

⁵<http://www.ska.ac.za/meerkat/>

⁶<http://www.atnf.csiro.au/projects/askap/index.html>

(2013). Both instruments will allow much deeper radio observations of the southern sky than was hitherto possible.

On a longer time scale, the Square Kilometer Array (SKA⁷) will be built, providing a further order of magnitude improvement in sensitivity compared with the EVLA. SKA is expected to have 10 % of its capability in 2016-2019 with full capability by 2024. Much closer in time is the Atacama Large Millimeter Array (ALMA⁸), consisting of 66 antennas, covering the wavelength range 350 μm – 9 mm. Early science will start in 2011, with full operations in 2013.

5 Conclusions

The simple relation between thermal radio emission and mass-loss rate was thought to give us a reliable set of mass-loss rates for hot, massive stars. Unfortunately, the presence of clumping in the wind makes this impossible at the moment. The radio data are very useful however as a reference point to determine the amount of clumping in the inner wind. From this we learned that there is a clumping gradient in strong stellar winds, with the clumping decreasing as we move further away from the star. It is important to realize that, out of necessity, it is assumed there is no clumping in the radio formation region. It should be realized however that the radio region is probably clumped as well.

For the non-thermal radio emission, it is now clear that this is due to colliding-wind binaries, both for Wolf-Rayet and O stars. The variations in the observed radio light curve are due to a combination of intrinsically varying synchrotron emission (in an eccentric binary) and the varying free-free absorption along the sightline to the observer. The study of these colliding-wind systems is important for a number of reasons: we can learn more about the Fermi mechanism that accelerates the electrons, which is also relevant in other astrophysical contexts; colliding-wind binaries help in the binary frequency determination in clusters; and they can provide constraints on clumping and porosity in stellar winds. This last constraint depends on the development of good models for the observations. Such modelling work is quite challenging, as it has to explain not only the radio data, but also the X-ray and optical spectroscopy observations.

Finally, radio instrumentation is currently being upgraded and new facilities are planned for the near future. For the study of radio emission from hot, massive stars, this will provide a step forward that is at least as big as the introduction of the VLA was, some 30 years ago.

Acknowledgements

I would like to thank my colleagues who collaborated with me on this interesting subject of radio observation of massive stars, especially M. De Becker, R. K. Prinja, G. Rauw, M. C. Runacres, J. Vandekerckhove, S. Van Loo and D. Volpi.

References

- Abbott, D. C., Bieging, J. H., Churchwell, E., & Cassinelli, J. P. 1980, ApJ, 238, 196
- Abbott, D. C., Bieging, J. H., & Churchwell, E. 1981, ApJ, 250, 645
- Abbott, D. C., Bieging, J. H., & Churchwell, E. 1984, ApJ, 280, 671
- Abbott, D. C., Bieging, J. H., Churchwell, E., & Torres, A. V. 1986, ApJ, 303, 239
- Bell, A. R. 1978, MNRAS, 182, 147

⁷<http://www.skatelescope.org/>

⁸<http://www.almaobservatory.org/>

- Benaglia, P. 2010, ASP Conf. Proc., 422, 111
- Benaglia, P., Cappa, C. E., & Koribalski, B. S. 2001, A&A, 372, 952
- Benaglia, P., Vink, J. S., Maíz Apellániz, J., et al. 2008, Rev. Mex. Astron. Astrofis. (Serie de Conferencias), 33, 65
- Bieging, J. H., Abbott, D. C., & Churchwell, E. B. 1982, ApJ, 263, 207
- Bieging, J. H., Abbott, D. C., & Churchwell, E. B. 1989, ApJ, 340, 518
- Blomme, R., Prinja, R. K., Runacres, M. C., & Colley, S. 2002, A&A, 382, 921
- Blomme, R., Van Loo, S., De Becker, M., et al. 2005, A&A, 436, 1033
- Blomme, R., De Becker, M., Runacres, M. C., Van Loo, S., & Setia Gunawan, D. Y. A. 2007, A&A, 464, 701
- Blomme, R., De Becker, M., Volpi, D., & Rauw, G. 2010, A&A, 519, A111
- Cappa, C. E., Goss, W. M., & Pineault, S. 2002, AJ, 123, 3348
- Cappa, C., Goss, W. M., & Van der Hucht, K. A. 2004, AJ, 127, 2885
- Chapman, J. M., Leitherer, C., Koribalski, B., Bouter, R., & Storey, M. 1999, ApJ, 518, 890
- Crowther, P. A. 2007, ARA&A, 45, 177
- De Becker, M. 2007, A&AR, 14, 171
- De Becker, M., Rauw, G., & Manfroid, J. 2004, A&A, 424, L39
- De Becker, M., Rauw, G., Sana, H., et al. 2006, MNRAS, 371, 1280
- Dougherty, S. M., & Williams, P. M. 2000, MNRAS, 319, 1005
- Dougherty, S. M., Beasley, A. J., Claussen, M. J., Zauderer, B. A., & Bolingbroke, N. J. 2005, ApJ, 623, 447
- Eichler, D., & Usov, V. 1993, ApJ, 402, 271
- Elitzur, M. 1992, *Astronomical Masers*, Astrophysics and space science library Vol. 170, Kluwer, the Netherlands
- Exter, K. M., Watson, S. K., Barlow, M. J., & Davis, R. J. 2002, MNRAS, 333, 715
- Kennedy, M., Dougherty, S. M., Fink, A., & Williams, P. M. 2010, ApJ, 709, 632
- Lamers, H. J. G. L. M., & Leitherer, C. 1993, ApJ, 412, 771
- Leitherer, C., Forbes, D., Gilmore, A. C., et al. 1987, A&A, 185, 121
- Leitherer, C., Chapman, J. M., & Koribalski, B. 1997, ApJ, 481, 898
- Marchenko, S. V., Moffat, A. F. J., Vacca, W. D., Côté, S., & Doyon, R. 2002, ApJ, 565, L59
- Moran, J. P., Davis, R. J., Spencer, R. E., Bode, M. F., & Taylor, A. R. 1989, Nature, 340, 449
- Morton, D. C., & Wright, A. E. 1978, MNRAS, 182, P47
- Nazé, Y., De Becker, M., Rauw, G., & Barbieri, C. 2008, A&A, 483, 543
- Nazé, Y., Damerdji, Y., Rauw, G., et al. 2010, ApJ, 719, 634
- Nugis, T., Crowther, P. A., & Willis, A. J. 1998, A&A, 333, 956
- Olnon, F. M. 1975, A&A, 39, 217
- Owocki, S. P., & Rybicki, G. B. 1984, ApJ, 284, 337
- Owocki S.P., Gayley K.G., & Shaviv N.J. 2004, ApJ, 616, 525
- Panagia, N., & Felli, M. 1975, A&A, 39, 1
- Paredes, J. M. 2009, ASP Conf. Proc., 407, 289
- Pittard, J. M., Dougherty, S. M., Coker, R. F., O'Connor, E., & Bolingbroke, N. J. 2006, A&A, 446, 1001
- Puls, J., Markova, N., Scuderi, S., et al. 2006, A&A, 454, 625
- Puls, J., Vink, J. S., & Najarro, F. 2008, A&AR, 16, 209
- Rohlfs, K. & Wilson, T. L. 2000, *Tools of radio astronomy*, 3rd ed., Astronomy and Astrophysics Library, Springer-Verlag, Berlin, Heidelberg, New York
- Runacres, M. C., & Blomme, R. 1996, A&A, 309, 544
- Runacres, M. C., & Owocki, S. P. 2005, A&A, 429, 323
- Seaquist, E. R., & Gregory, P. C. 1973, Nature, 245, 85
- Smith, N., & Owocki, S. P. 2006, ApJ, 645, L45
- Umana, G., Buemi, C. S., Trigilio, C., Leto, P., & Hora, J. L. 2010, ApJ, 718, 1036
- Van der Hucht, K. A., Williams, P. M., Spoelstra, T. A. Th., & De Bruyn, A. C. 1992, ASP Conf. Proc., 22, 249
- Van Loo, S., Runacres, M. C., & Blomme, R. 2006, A&A, 452, 1011
- Van Loo, S., Blomme, R., Dougherty, S. M., & Runacres, M. C. 2008, A&A, 483, 585
- Vink, J. S., De Koter, A., & Lamers, H. J. G. L. M. 2000, A&A, 362, 295
- Wendker, H. J., Baars, J. W. M., & Altenhoff, W. J. 1973, Nature, 245, 118
- Wendker, H. J., Smith, L. F., Israel, F. P., Habing, H. J., & Dickel, H. R. 1975, A&A, 42, 173
- White, R. L., & Becker, R. H. 1983, ApJ, 272, L19
- White, R. L., & Becker, R. H. 1995, ApJ, 451, 352
- Williams, P. M., Dougherty, S. M.; Davis, R. J., et al. 1997, MNRAS, 289, 10
- Wright, A. E., & Barlow, M. J. 1975, MNRAS, 170, 41